

Hydrogen peroxide measurements: its wet deposition in Higashi-Hiroshima city, concentration in Kurose River and role towards hydroxyl radical formation

*Anifowose A.J.¹, Olabode O.A.¹, Adedotun I.S.¹, Sakugawa H²

Abstract

Background: Hydrogen peroxide (H₂O₂) is a versatile reactive oxygen specie and a major source of hydroxyl radical (OH). The study was conducted to understand the production routes/sources, inter-relationship and roles of H₂O₂ and OH in the natural waters.

Method: The H₂O₂ and OH in rainwater and the Kurose River were measured monthly in the year 2013 using a HPLC-fluorescence detector.

Results: H₂O₂ concentrations in the rainwater and river were highly season-dependent. H₂O₂ concentrations in the rainwater varied from 0.03 μM (Winter) to 14.3 μM (Spring). Estimated wet deposition of H₂O₂ was 7.5 mmol m⁻² y⁻¹ while in the River, a range of 0.06–0.37 μM H₂O₂ were measured. The lowest and highest concentrations of H₂O₂ were found in the winter and summer, respectively. Good correlations existed between the solar intensity and H₂O₂ concentrations (rainwater: $r = 0.79$, $p < 0.01$; river: $r = 0.81$, $p < 0.01$) indicating photoproduction as a major H₂O₂ source in the natural waters.

Conclusion: H₂O₂ was a major OH source in the rainwater (0.2–48%), while NO₂⁻ was predominantly OH source (49–80%) in the Kurose River.

Keywords

rainwater; river; photoproduction; radical; deposition; reactive oxygen species

*Corresponding author

Anifowose A.J.

Email: adebanjo.anifowose@uniosun.edu.ng

¹Department of Pure and Applied Chemistry, Faculty of Basic and Applied Sciences, Osun State University, Osogbo, Nigeria

²Graduate School of Integrated Sciences for Life, Hiroshima University, 1-7-1 Kagamiyama, Higashi-Hiroshima, 739-8521, Japan

Received: August 30, 2021

Accepted: September 24, 2021

Published: December 30, 2021

Research Journal of Health Sciences subscribed to terms and conditions of Open Access publication. Articles are distributed under the terms of Creative Commons Licence (CC BY-NC-ND 4.0). (<http://creativecommons.org/licenses/by-nc-nd/4.0>).

<http://dx.doi.org/10.4314/rejhs.v9i4.8>

L'hydrogène peroxyde mesures: le dépôt humide dans la ville de Higashi-Hiroshima, la concentration en rivière et Kurose rôle vers formation radicale hydroxyle

*Anifowose A.J.¹, Olabode O.A.¹, Adedotun I.S.¹, Sakugawa H²

Résumé

Contexte général l'étude: Le peroxyde d'hydrogène (H_2O_2) est une espèce d'oxygène réactif polyvalente et une source majeure de radicaux hydroxyles (OH). L'étude a été menée pour comprendre les voies/sources de production, les interrelations et les rôles de H_2O_2 et OH dans les eaux naturelles.

Méthode de l'étude : Le H_2O_2 et OH dans les eaux de pluie et la rivière Kurose ont été mesurés mensuellement en 2013 à l'aide d'un détecteur HPLC-fluorescence.

Résultat de l'étude: Les concentrations d' H_2O_2 dans l'eau de pluie et la rivière étaient fortement dépendantes de la saison. Les concentrations d' H_2O_2 dans l'eau de pluie variaient de 0,03 M (hiver) à 14,3 M (printemps). Le dépôt humide estimé d' H_2O_2 était de 7,5 mmol m⁻² an⁻¹ tandis que dans la rivière, une fourchette de 0,06–0,37 M H_2O_2 a été mesurée. Les concentrations les plus faibles et les plus élevées d' H_2O_2 ont été trouvées en hiver et en été, respectivement. De bonnes corrélations existaient entre l'intensité solaire et les concentrations de H_2O_2 (eau de pluie : $r = 0,79$, $p < 0,01$; rivière : $r = 0,81$, $p < 0,01$) indiquant la photo production comme source majeure de H_2O_2 dans les eaux naturelles.

Conclusion : H_2O_2 était une source majeure de OH dans l'eau de pluie (0,2–48 %), tandis que le NO_2 était principalement une source de OH (49–80 %) dans la rivière Kurose.

Mots -clés : Eau de pluie, fleuve, photo-fabrication; radical, déposition, les espèces réactives de l'oxygène

*Corresponding author

Anifowose A.J.

Email: adebanjo.anifowose@uniosun.edu.ng

¹Department of Pure and Applied Chemistry, Faculty of Basic and Applied Sciences, Osun State University, Osogbo, Nigeria

²Graduate School of Integrated Sciences for Life, Hiroshima University, 1-7-1 Kagamiyama, Higashi-Hiroshima, 739-8521, Japan

Received: August 30, 2021

Accepted: September 24, 2021

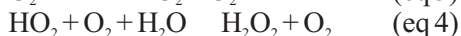
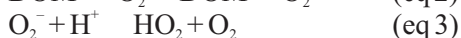
Published: December 30, 2021

Research Journal of Health Sciences subscribed to terms and conditions of Open Access publication. Articles are distributed under the terms of Creative Commons Licence (CC BY-NC-ND 4.0). (<http://creativecommons.org/licenses/by-nc-nd/4.0>).

<http://dx.doi.org/10.4314/rejhs.v9i4.8>

INTRODUCTION

Hydrogen peroxide (H_2O_2) is a highly soluble reactive oxygen specie (ROS) that possesses both reducing and oxidizing potentials in natural waters. Its high solubility and consequent dissolution from the gas phase into the aqueous phase in the atmosphere makes H_2O_2 readily available in rainwater. Other route to its production in the atmospheric aqueous phase is thought to be by the reaction of hydro-peroxide with superoxide ($\text{HO}_2 + \text{O}_2^- + \text{H}_2\text{O} \rightarrow \text{H}_2\text{O}_2 + \text{O}_2 + \text{OH}^-$). H_2O_2 is a source of hydroxyl radical (OH), and influences the photo-productions of other reactive oxygen species such as hydro-peroxide radical (HO_2) and organo-peroxide radical (RO_2) in the atmosphere (1). Among the ROS (including nitric oxide, NO, and superoxide, O_2^-), and in respect to dark decay processes, H_2O_2 relatively has longer lifetime (order of hours). H_2O_2 has been reported to actively mediate in the conversion of dissolved SO_2 to SO_4^{2-} at $\text{pH} < 5$ in atmospheric water droplet (2), thereby contributing to rainwater acidity. H_2O_2 and OH could play major roles in the aqueous-phase oxidation of aldehydes to produce organic acids in the atmosphere (3). Owing to its influential contribution to acid rain, high concentration of H_2O_2 in either gas or aqueous phase of the atmosphere could lead to deforestation. In rainwater, its concentration has been reported to range from nanomolar to micromolar (3,4,5,6,7).



Other H_2O_2 sources in the surface waters include biological processes, wet and dry depositions. Some of the organic sources in river water include humic substances, coloured dissolved organic matter and fluorescent dissolved organic matter. These could all absorb radiation photons from sunlight to undergo photochemical transformations, thereby producing H_2O_2 . The presence of H_2O_2 could affect the biogeochemical fate and dynamics of the resident redox-active chemical species in river water due to its reducing and oxidizing potentials. As a good source of OH, H_2O_2 could therefore mediate in the photodegradation of some recalcitrant organic compounds in natural river.

Hydroxyl radical is the most important ROS in the gas phase. Photochemical processes involving photolysis of H_2O_2 , $\text{NO}_2^-/\text{HNO}_2$, NO_3^- and DOM generate OH in the atmosphere (8) and

surface waters. A study by (7) showed atmospheric OH production in the aqueous-phase by photo-Fenton reaction. In river waters, evidence of OH photoformation has been reported in literatures (7,9,10). One of the major OH roles in river water is the degradation of recalcitrant organic compounds as reported earlier (11,12).

There is need to have seasonal data and simultaneous study on H_2O_2 (as well as OH) produced in both the rainwater and Kurose River in Higashi-Hiroshima (Hiroshima Prefecture), Japan. This is due to the strategic location of the city (see Figure 1) and Kurose River runs across the entire city. Kurose River is about 43 km long and it empties into the Seto Inland Sea; the Sea contributes to the seafood supply of the country. The city has a population of about 184,000 (10) with numerous rice and other agricultural fields. This study, therefore, investigated monthly H_2O_2 and OH productions in rainwater and the Kurose River in the city. Findings in this study would give valuable information on the amount of annual wet deposition of H_2O_2 in the city, its role as a OH photochemical source in the rainwater and Kurose River in the city, its seasonal variations in both natural waters and consequent roles in the aqueous environment.

MATERIALS AND METHODS

Reagents

Milli-Q water with electrical resistivity of $>18.2 \text{ M}\Omega \text{ cm}$ (Millipore, Japan) was used appropriately in all the experiments. H_2O_2 was purchased from Sigma Aldrich, Japan. Phenol, benzene and acetonitrile were supplied by Nacalai Tesque Inc., Japan. Sulphuric acid was obtained from Sigma-Aldrich, Japan. Iron (II) sulphate pentahydrate was purchased from Nacalai Tesque (Guaranteed Reagent). Reagent standards of anions: NO_2^- , NO_3^- , Cl^- and SO_4^{2-} , and cations: NH_4^+ , Na^+ , K^+ , Ca^{2+} and Mg^{2+} , were purchased from Nacalai Tesque Inc., Japan. All other reagents were of analytical grade.

Sampling

Rainwater was collected every month on the roof-top of the building of Faculty of Integrated Arts and Science, Hiroshima University in Higashi-Hiroshima city, Japan ($34^\circ 24' \text{N}$, $132^\circ 42' \text{E}$; altitude = 242 m above the sea level). Sampling was carried out between January and December, 2013, into a clean 2 L polyethylene (PE) bottle through a PE funnel (opening diameter = 24 cm). The sampling bottle and funnel were set out for rain collection just

before a precipitation event and transported to the laboratory immediately after the precipitation. It is important to mention that rain sample could not be collected in July and September, 2013.

Surface water was collected from the Kurose River, in each month (January and December 2013) at six different locations. The locations were Namitakiji (the upstream), Tokumasa, Izumi, Ochiai, Hinotsume and Kurose Bunka Center (the downstream). Samples were collected with high density polyethylene bucket and stored in 1 L amber glass bottles. For each sampling event in the river, there was no precipitation at least 48 h before the sampling. Filtration followed immediately in the laboratory using a pre-combusted glass fiber filter (GC 50, Advantech). Detailed descriptions of Kurose River and these sampling locations have been published by our group (10). All the water samples (rain and river) were filtered with pre-combusted glass fibre filter (GC 50, Advantech) and were stored in the dark at 4 °C for other analyses. The map showing sampling locations of the rainwater and in the Kurose River is given in Figure 1.

H₂O₂ Analysis

Measurements of H₂O₂ in both the rain and river waters were completed less than 1 h after each sampling. Measurements were carried out according to the method reported by Olasehinde et al. (13). In brief, a stock solution of 20 mM benzene was prepared in Milli-Q water. Standard H₂O₂ concentrations were prepared by the appropriate dilution of the stock solution (1 mM H₂O₂) with milli-Q water. The stock solution was prepared daily from the commercially available H₂O₂ reagent (30%, w/v). The concentration of the commercially available H₂O₂ reagent was first determined by measuring the absorbance (using UV-2400PC spectrophotometer, Shimadzu) of 1000 fold dilution of the H₂O₂ at 240 nm in a 1 cm cell. Using the molar extinction coefficient of H₂O₂ ($\epsilon = 38.1 \text{ Lmol}^{-1} \text{ cm}^{-1}$) (14), the concentration of the H₂O₂ reagent was determined. Acidified 0.1 M Fe²⁺ was prepared in 0.07 M H₂SO₄. Aliquots of benzene and then Fe²⁺ were added to 3 mL of filtered sample (or H₂O₂ standard solution) in a 5 mL amber glass bottle to give final concentrations of 1.2 mM and 1.54 mM, respectively. After 5 min reaction time, the phenol produced was separated by a HPLC and measured at 270/298 nm (excitation/emission wavelengths) using a fluorescent detector. The HPLC used reverse-phase column (Supelco, LC-18: 5 μm , 4.6 mm i.d. x 250 mm length), while the

detector was interfaced with a C-R6A Chromatopac integrator (Shimadzu, Japan). The mobile phase was acetonitrile:Milli-Q (1:1, v/v) at a flow rate of 1 mL min⁻¹. The detection limit for H₂O₂ measurement in the rain and river water was 6 nM – defined as 3 σ of the lowest standard H₂O₂ concentration.

Photochemical OH Measurement

Photochemical measurement of OH in the irradiated samples (river and rainwater) was conducted according to previous reports (9,10). Benzene was used as a chemical probe for the radical, while the photochemical experiment was carried out with the aid of a OH radical auto-analyzer reported by (7). A HPLC attached to the OH auto-analyzer was equipped with a fluorescence detector (operated at 270/298 nm for excitation/emission wavelengths). A reverse-phase column (Supelco, LC-18: 5 μm , 4.6 mm i.d. x 250 mm length) interfaced with a C-R6A Chromatopac integrator (Shimadzu, Japan) was used. The mobile phase was an acetonitrile:Milli-Q mixture (1:1, v/v) while the flow rate was 1 mL min⁻¹.

An aliquot of each river sample (about 7.5 mL), containing 1.2 mM benzene in a quartz cell, was irradiated for 40 min using the solar simulator. During irradiation, samples were withdrawn at 10 min intervals and analyzed for phenol (product of benzene reaction with the OH) by the HPLC. For accurate quantification, phenol standards were analyzed during each experiment. The retention time of phenol was 5.5 min and the phenol standards were found to be linear up to 200 nM. The photoformation rate of OH (R_{OH}) was determined using equation 5.

$$R_{\text{OH}} = \frac{R_{\text{phenol}}}{Y_{\text{phenol}} \times F_{\text{benzene-OH}}} \quad (\text{eq 5})$$

where R_{phenol} is the photoformation rate of phenol in the sample, Y_{phenol} is the yield of phenol formed in the reaction between benzene and OH, and $F_{\text{benzene-OH}}$ is the fraction of OH that reacts with benzene. A Y_{phenol} value of 0.75, as reported earlier (15) was used in all the calculations. This value has been used for river and rain water by previous investigators (7). The $F_{\text{benzene-OH}}$ values determined experimentally in this study for the river samples were in the range of 0.90 and 0.99, while that of the rainwater were in the range of 0.91–0.99. Therefore, an average value of 0.95 was used for $F_{\text{benzene-OH}}$ in all R_{OH} calculations.

To determine the steady-state concentrations of OH, a plot of the inverse of R_{phenol} against that of the various concentrations of

benzene for each sample was found to be linear (equation 6). Therefore, benzene was added to different aliquots of each sample and the final concentrations of benzene were 25, 50, 75 and 100 μM . These were subsequently irradiated in the OH auto-analyzer for 40 min with aliquots being withdrawn at 10 min intervals for phenol analysis by the HPLC.

$$\frac{I}{R_{\text{phenol}}} = \frac{K'_{\text{scavenger}}}{R_{\text{OH}} \times Y_{\text{phenol}} \times K_{\text{benzene}}} \left(\frac{I}{[\text{benzene}]} \right) + \frac{I}{R_{\text{OH}} \times Y_{\text{phenol}}} \quad (\text{eq 6})$$

A k_{benzene} (second order reaction rate between benzene and OH) value of $7.8 \times 10^9 \text{ M}^{-1} \text{ s}^{-1}$ was used (7,16). The intercept of the graph is $1/(R_{\text{OH}} \times Y_{\text{phenol}})$ while $k'_{\text{scavenger}}$ is the scavenging rate constant for all the OH natural scavengers in the sample.

The scavenging rate constant for all the OH natural scavengers was determined using equation 7, while the steady-state concentration ($[\text{OH}]_{\text{ss}}$) and lifetime ($\text{lifetime}_{\text{OH}}$) of OH were determined using equations 8 and 9, respectively:

$$K'_{\text{scavenger}} = \frac{\text{slope} \times K}{\text{intercept}} \quad (\text{eq 7})$$

$$[\text{OH}]_{\text{ss}} = \frac{\text{rate of } \cdot\text{OH production}}{\text{rate of } \cdot\text{OH scavenging}} = \frac{R_{\text{OH}}}{K'_{\text{scavenger}}} \quad (\text{eq 8})$$

$$\text{lifetime}_{\text{OH}} = \frac{1}{K'_{\text{scavenger}}} \quad (\text{eq 9})$$

The daily actinic fluxes of the solar simulators used were determined from the photolysis rate constant of 8 μM 2-nitrobenzaldehyde (2-NB) photodegradation by the solar simulators. The photolysis rate constants of 8 μM 2-NB during OH study ranged between 0.0093 and 0.0105 s^{-1} . All data relating to the photochemical reactions were normalized to a 2-NB photodegradation rate of 0.0093 s^{-1} , as determined at noon under ambient sky conditions in Higashi-Hiroshima on May 1, 1998 (15).

Other Measurements

Temperatures of all the samples were taken during sampling. The concentrations of major anions (NO_2^- , NO_3^- , Cl^- and SO_4^{2-}) and cations (NH_4^+ , Na^+ , K^+ , Ca^{2+} and Mg^{2+}) in both the rain and river samples were measured by ion chromatography (Dionex ICS-1600). The mobile phases for the anions and cations analyses were 20 mM methyl sulphonic acid and 20 mM $\text{Na}_2\text{CO}_3/1 \text{ mM NaHCO}_3$, respectively. Standards solutions of the anions and cations were prepared by appropriate dilutions from their commercially available standard solutions. Dissolved organic carbon (DOC) in all the samples was measured by

high temperature combustion using a TOC- V_{CSH} analyzer (Shimadzu, Japan) equipped with ASI autosampler. The DOC standard solutions were prepared from potassium hydrogen phthalate. Each sample was injected three times with a relative standard deviation (RSD) 3%.

RESULTS AND DISCUSSION

Concentrations of H_2O_2 in the Rainwater and Kurose River

There were marked differences in H_2O_2 concentrations, measured in the two natural waters. The rainwater H_2O_2 concentrations varied widely from 0.03 μM in February to as high as 14.3 μM in May (Figure 2a). These results are consistent with the previous measurements (0.77–13.9 μM) in Higashi-Hiroshima city (7). Analysis of H_2O_2 in Sao Paulo rainwater (17) and Los Angeles rainwater (3) showed similar wide variation, ranging 0.5–78 μM and 0.01–145 μM , respectively. The 3-order magnitude of increment from winter to spring in this study could be attributed to the prevailing atmospheric constituents and weather conditions during the rainfall. The temperature of the February sample was 3.5 $^\circ\text{C}$, whereas that of May was 16.5 $^\circ\text{C}$ (Table 1). It has been established that H_2O_2 concentration in the atmosphere is usually high in the summer and afternoon, while low concentration is found in the winter and at night (18, 19, 20). Therefore, it is conceivable that the high H_2O_2 concentration in the summer rain could be due to considerable dissolution from the gas-phase, considering the high solubility of H_2O_2 in water.

The detailed results of major ions measured in the samples are contained in Tables 2 and 3. Among the measured anions, SO_4^{2-} concentration was highest (0.8–35, av = 18.2 μM). This was followed by that of Cl^- and NO_3^- , while NO_2^- had the lowest concentration. Previous anions data in the rainwater (7) and aqueous solution of water-soluble gases (8) from the same sampling area of the city confirmed similar trend. This indicates consistent trend in concentrations of the atmospheric anions present in the city over the years. H_2O_2 has been reported (21) as a major oxidant for SO_2 (forming SO_4^{2-}) in the atmospheric liquid phase at $\text{pH} < 5$. In the months of March and April, $\text{pH} < 5$ were measured in the rainwater; this shows that SO_2 may not be a dominant factor controlling the fate of the atmospheric H_2O_2 during this period in the city. The reported pH of rainwater in Turin (Italy) ranged 4.4–6.6 (22), while that of rainwater in Los Angeles was in the range of 4.5–6.4 (3).

The H_2O_2 measurements in the Kurose River (average of six locations) were of about 1 order of magnitude in variation, 0.06–0.37 μM , throughout the 12-month study (Figure 2b). The average concentrations in the year showed that H_2O_2 was produced more in the rainwater ($[\text{H}_2\text{O}_2] = 4.38 \mu\text{M}$) than in the river ($[\text{H}_2\text{O}_2] = 0.13 \mu\text{M}$). Considering the rainwater downpour and its high H_2O_2 constituent, there was high possibility that the H_2O_2 concentrations measured in the Kurose River were influenced by wet deposition.

Seasonal H_2O_2 variations in the rainwater and Kurose River showed that winter period (December–February) produced the lowest H_2O_2 concentrations in the two natural waters (Figure 3). In the rainwater, highest H_2O_2 concentrations were present during the spring (March–May) (Figure 3a). It should be noted that the average H_2O_2 concentration in rainwater measured in the summer (June–August) would be influenced by lack of July data (the peak of summer) sample in the year. This could be justified by the highest H_2O_2 concentration (0.37 μM) measured in July in the Kurose River (Figure 2b). Nevertheless, the current results with highest (10.3 μM) and lowest (0.2 μM) H_2O_2 concentrations in the spring and winter rain, respectively, are of similar seasonal trend when compared with results from other countries (17,23). The higher H_2O_2 concentrations in the spring rain could be attributed to higher volatile organic compounds (VOC) emission to the atmosphere, as facilitated by intense solar radiation. The VOC emission in the spring would be made easier by soil tillage for rice planting and other agricultural activities that characterized this season in Japan. VOC emission from the vegetation in the planting season could be an additional plausible factor to the higher H_2O_2 in the spring. The possibility of more VOC emission to the atmosphere in the spring is justified by the dissolved organic carbon (DOC) measured in the samples (Table 2). While an average DOC concentration of 104 μM (carbon) was measured in spring, the DOC in winter was 65.7 μM (carbon). Similarly in the Kurose River, highest H_2O_2 concentration (0.20 μM ; Figure 3.3) was present in the summer (closely followed by 0.15 μM measured in spring), whereas a low 0.06 μM was measured in the winter. Similar study by (24) supported this seasonal trend in the H_2O_2 concentrations measured in the Kurose and Ohta Rivers (located in the same Prefecture as the Kurose River). In this study, high solar intensity that characterized spring and summer would be a major factor responsible for the high H_2O_2 concentrations measured in the Kurose River

during the two seasons. This is because the formation of H_2O_2 in natural waters is greatly influenced by the natural solar intensity (24). To investigate this, average solar intensity during the hours of the precipitations was plotted against the measured H_2O_2 in the rainwater samples. For the Kurose River, average solar intensity of six hours prior to the sampling time was plotted against the H_2O_2 concentration measured. The plots showed that a good positive correlation existed between the solar intensity and H_2O_2 concentration measured in both the rainwater ($r = 0.79$, $p < 0.01$) and in the Kurose River ($r = 0.81$, $p < 0.01$) (Figure 4).

Flux of H_2O_2 in the Rainwater and Kurose River

The average volume-weighted H_2O_2 concentration in rainwater in the studied year (2013) was 4.17 μM . According to the online data by Japan Meteorological Agency (<http://www.data.jma.go.jp/obd/stats/etrn/>), the total precipitation in the year 2013 in Higashi-Hiroshima city was 1708 mm. With 310 mm total precipitation event involved in this study, about 18% of the year precipitation was measured. Though this proportion might not be sufficient to accurately discuss H_2O_2 flux in the entire year, it is still relevant to understanding H_2O_2 deposition and dynamics in the city. By calculation, an average of 7.48 (range, 0.05–24.4) $\text{mmol H}_2\text{O}_2 \text{ m}^{-2} \text{ y}^{-1}$ was estimated to have been deposited in 2013 by wet deposition in the city. This value is consistent with the average H_2O_2 wet deposition rate of 6.85 (range, 4.0–10.8) $\text{mmol m}^{-2} \text{ y}^{-1}$ in Hiroshima prefecture (in which Higashi-Hiroshima city is located) by previous investigators (25). Also, the current estimation is similar to findings by Yamada et al (26) who reported annual wet deposition of H_2O_2 in Kyoto city (Japan) to be 11.7 and 9.11 $\text{mmol m}^{-2} \text{ y}^{-1}$ for the year 1999 and 2000, respectively. Their calculations were based on volume-weighted averages of 7.47 and 6.70 $\mu\text{M H}_2\text{O}_2$ measured in the city's rainwater in 1999 and 2000, respectively. Wet deposition of 1.5 $\text{mmol H}_2\text{O}_2 \text{ m}^{-2} \text{ y}^{-1}$ was reported in Los Angeles (3) with average rainfall of 340 mm y^{-1} . Similarly in a coastal southern USA city (Wilmington, North Carolina), the annual deposition of H_2O_2 by rain was measured to be 12 $\text{mmol m}^{-2} \text{ y}^{-1}$ (average volume-weighted $\text{H}_2\text{O}_2 = 9.6 \mu\text{M}$; annual rainfall = 1.3 m) (27). The measured wet deposition of H_2O_2 in this study could impact on the ocean dynamics as H_2O_2 has been reported to be toxic to cyanobacterium *Prochlorococcus* even at

relevant environmental concentrations (28) and also implicated in the oxidative stress of marine organisms (29). The deposition of H_2O_2 to the surface waters would influence the metal speciation (being an oxidizing and reducing agent), which consequently affect their bioavailability to the resident biota in the aquatic surface environment.

The flux of H_2O_2 in the Kurose River was also estimated. The flux was calculated only for Hinotsume station where data on daily water depth is available from Hiroshima Prefecture Office. A plot of water flow rate against water depth at this station gave an equation: $y = 4.68x + 4.24$ ($r^2 = 0.78$) (30). Water depths for the sampling days during the twelve-month study were in the range of -0.58–0.01 m. Therefore, the estimated flow rates at Hinotsume were in the range of 1.53 – $4.29 \text{ m}^3 \text{ s}^{-1}$ with an annual average of $2.1 \text{ m}^3 \text{ s}^{-1}$. This is consistent with an annual average of $1.9 \text{ m}^3 \text{ s}^{-1}$ reported earlier for the Kurose River (31). H_2O_2 flux at this station was calculated as a product of H_2O_2 concentration and the flow rate. The results are shown in Figure 5. The lowest H_2O_2 flux (0.08 mmol s^{-1}) was recorded in December, apparently due to the lowest river flow rate ($1.53 \text{ m}^3 \text{ s}^{-1}$) and moderately low H_2O_2 concentration ($0.05 \mu\text{M}$). However, high flow rate ($4.29 \text{ m}^3 \text{ s}^{-1}$) due to heavy rainfall in addition to moderately high H_2O_2 concentration ($0.13 \mu\text{M}$) resulted in the highest H_2O_2 flux (0.56 mmol s^{-1}) in June. On the average, H_2O_2 flux at this station in the river was estimated to be 0.22 mmol s^{-1} . As shown in Figure 5 (inset), the amount of H_2O_2 transported per time in the river has positive relationship with the river flow rate ($p < 0.01$; $r = 0.73$). Similarly, there was a significant positive relationship ($p < 0.05$; $r = 0.67$) between concentration and flux of H_2O_2 in the river.

Hydroxyl Radical and H_2O_2 Contribution towards its Photochemical Production in the Rainwater and Kurose River

The photochemical measurements of the hydroxyl radical (OH) generated during solar irradiation of rainwater and Kurose River samples produced marked differences. Average OH measurements of the six locations in the river are considered in this study. The OH photoformation rates in the river water, (0.7 – 5.1) $\times 10^{-10} \text{ M s}^{-1}$, was about 1 order of magnitude higher than those measured in the rainwater (in the order of $10^{-11} \text{ M s}^{-1}$), except for the December rainwater (Table 4). The exceptionally high nitrite concentration ($1.36 \mu\text{M}$) in the December rain was responsible for the high OH

photoformation rate ($23.6 \times 10^{-11} \text{ M s}^{-1}$) measured in the month. The six-month OH photochemical measurement in rainwater by (7) and (22) produced lower photoformation rates, (2.5 – 11.8) $\times 10^{-11} \text{ M s}^{-1}$ and (2.0 – 6.5) $\times 10^{-11} \text{ M s}^{-1}$, respectively. In the Kurose River, the highest nitrite concentration ($15.2 \mu\text{M}$) was measured in May, thus producing the highest OH photoformation rate ($5.1 \times 10^{-10} \text{ M s}^{-1}$) measured in the year. Leachates from the agricultural fields due to peak farming activities around the river in May could be responsible for the relatively high nitrite content in the month.

To further investigate the potentials of various sources of OH photoformation in the natural waters, contributions from H_2O_2 , NO_2^- and NO_3^- were calculated using the relationship in equation 10. The results of anions and cations measured in the samples are contained in Table 2.

$$\text{Contribution (\%)} = (\text{J}_{\text{OH}i} \times [i] \times 100) / \text{R}_{\text{OH}}$$

R_{OH} (M s^{-1}) is the OH photoformation rate, $[i]$ is the molar concentration (M) of H_2O_2 , NO_2^- or NO_3^- in the water sample and $\text{J}_{\text{OH}i}$ is the photoformation rate constant of OH from “i” ($i = \text{H}_2\text{O}_2$, NO_2^- or NO_3^-) solution under solar irradiation. The $\text{J}_{\text{OH}i}$ values reported by Takeda et al (9) under such conditions ($\text{J}_{\text{OH}i\text{H}_2\text{O}_2} = 4.02 \times 10^{-6} \text{ s}^{-1}$; $\text{J}_{\text{OH}i\text{NO}_2} = 2.30 \times 10^{-5} \text{ s}^{-1}$; $\text{J}_{\text{OH}i\text{NO}_3} = 1.60 \times 10^{-7} \text{ s}^{-1}$) were used in this study. In the rainwater, H_2O_2 and the unknown source were the dominant sources of the OH photochemical production, contributing 0.2–48% (av = 24%) and 43–84% (av = 62%), respectively (Table 5). It is important to state that the least H_2O_2 contributions, 0.2–5.9% (av = 2.2%), were in the winter. Nakatani et al. (7) reported a higher H_2O_2 contribution towards the R_{OH} (3–74%, av = 37%) due to the absence of winter data. A significant portion of the R_{OH} contribution by the unknown source could be added to photo-Fenton reaction; Nakatani et al. (7) reported 5–38% contribution by photo-Fenton reaction towards OH photoformation rate in the city's rainwater. Though the rate constant for the OH formation from H_2O_2 photolysis in aqueous solution under sunlight was ~1 order of magnitude lower than that from NO_2^- , the significant H_2O_2 contributions towards OH photoformation rate in the rainwater was made possible by its high H_2O_2 concentrations. The published values of 69–138% NO_2^- contributions towards OH photoformation rate (22) in rainwater is in contrast to findings in this study as only 2–29% contribution by NO_2^- towards OH photoformation rate were estimated.

Unlike the OH photochemical

measurement in the rainwater, nitrite was the major OH source in the Kurose River due to its higher concentrations in the river, while contributions by the H_2O_2 was somewhat negligible (0.1–0.7%). Similar investigations by Nakatani et al. (7) and Takeda et al. (9) confirmed nitrite as one of the dominant OH photochemical sources in river waters with estimated contributions in the range of 1–89% and 6–80%, respectively, while <1% of the OH photoformation rate was accounted for by H_2O_2 . According to Nakatani et al. (7), 2–29% of the OH photoformation in the Kurose River was as a result of photo-Fenton reaction. Nitrate contributions towards OH photoformation were apparently similar (<9%) in both the natural waters. Hence, nitrate is not a major OH photoformation source in the rainwater and Kurose River. The estimated lifetimes of OH in the rainwater and Kurose River were 1.0–10 (av, 3.6) μ s and 1.1–13 (av, 4.8) μ s, respectively, indicating that the order of reactivity of OH in the two natural waters are similar.

CONCLUSIONS

The study showed that H_2O_2 concentrations in the rainwater and Kurose River of Higashi-Hiroshima were seasonal. Winter season produced the lowest concentrations in the natural waters. Solar intensity is an important factor in the production of H_2O_2 in natural waters. H_2O_2 is a major production source of OH in rainwater, while nitrite is the major OH source in the Kurose River of Higashi-Hiroshima city.

Conflict of Interest: The authors declare no conflict of interest.

Acknowledgements: Appreciation to Dr Chikumbusko Chiziwa Kaonga (Department of Physics and Biochemical Sciences, University of Malawi) for his support during the sampling of the river water used in this study.

REFERENCES

1. Gunz DW, Hoffmann MR. Atmospheric chemistry of peroxides: a review. *Atmospheric Environment*. 1990;24A:1601–1633.
2. Fung CS, Misra PK, Bloxam R, Wong S. A numerical experiment on the relative importance of H_2O_2 O_3 in aqueous conversion of SO_2 to SO_4^{2-} . *Atmospheric Environ. Part A*. 1991;25(2):411-23
3. Sakugawa H, Kaplan IR, Shepard LS. Measurements of H_2O_2 , aldehydes and organic acids in Los Angeles rainwater: their sources and deposition rates. *Atmospheric Environment. Part B. Urban Atmosphere*. 1993;27(2):203-19.
4. Deng Y, Zuo Y. Factors affecting the levels of hydrogen peroxide in rainwater. *Atmospheric Environment*. 1999;33(9):1469-78.
5. Yuan J, Shiller AM. The variation of hydrogen peroxide in rainwater over the South and Central Atlantic Ocean. *Atmospheric Environment*. 2000;34(23):3973-80.
6. Peña RM, García S, Herrero C, Lucas T. Measurements and analysis of hydrogen peroxide rainwater levels in a Northwest region of Spain. *Atmospheric Environment*. 2001;35(2):209-19. [https://doi.org/10.1016/S1352-2310\(00\)00246-6](https://doi.org/10.1016/S1352-2310(00)00246-6)
7. Nakatani N, Ueda M, Shindo H, Takeda K, Sakugawa H. Contribution of the photo-Fenton reaction to hydroxyl radical formation rates in river and rain water samples. *Analytical Sciences*. 2007;23(9):1137-42.
8. Nomi SN, Kondo H, Sakugawa H. Photoformation of OH radical in water-extract of atmospheric aerosols and aqueous solution of water-soluble gases collected in Higashi-Hiroshima, Japan. *Geochemical Journal*. 2012;46(1):21-9.
9. Takeda K, Takedoi H, Yamaji S, Ohta K, Sakugawa H. Determination of hydroxyl radical photoproduction rates in natural waters. *Analytical sciences*. 2004;20(1):153-8.
10. Anifowose AJ, Takeda K, Sakugawa H. Photoformation rate, steady-state concentration and lifetime of nitric oxide radical (NO) in a eutrophic river in Higashi-Hiroshima, Japan. *Chemosphere*. 2015;119:302-9.
11. Brezonik PL, Fulkerson-Brekken J. Nitrate-induced photolysis in natural waters: controls on concentrations of hydroxyl radical photo-intermediates by natural scavenging agents. *Environmental Science & Technology*. 1998;32(19):3004-10.
12. Olasehinde EF, Hasan N, Omogbehin SA, Kondo H, Sakugawa H. Hydroxyl radical mediated degradation of diuron in river water. *The Journal of American Science*. 2013;9(4):29-34.
13. Olasehinde EF, Makino S, Kondo H, Takeda K, Sakugawa H. Application of Fenton

- reaction for nanomolar determination of hydrogen peroxide in seawater. *analytica chimica acta*. 2008;627(2):270-6.
14. Miller WL, Kester DR. Hydrogen peroxide measurement in seawater by (p-hydroxyphenyl) acetic acid dimerization. *Analytical Chemistry*. 1988;60(24):2711-5.
 15. Arakaki T, Faust BC. Sources, sinks, and mechanisms of hydroxyl radical (OH) photoproduction and consumption in authentic acidic continental cloud waters from Whiteface Mountain, New York: The role of the Fe (r(= II, III) photochemical cycle. *Journal of Geophysical Research: Atmospheres*. 1998;103(D3):3487-504.
 16. Buxton GV, Greenstock CL, Helman WP, Ross AB. Critical review of rate constants for reactions of hydrated electrons, hydrogen atoms and hydroxyl radicals (OH/O^- in aqueous solution. *Journal of physical and chemical reference data*. 1988;17(2):513-886.
 17. Gonçalves C, Santos MA, Fornaro A, Pedrotti JJ. Hydrogen peroxide in the rainwater of Sao Paulo megacity: measurements and controlling factors. *Journal of the Brazilian Chemical Society*. 2010;21(2):331-9.
 18. Dasgupta PK, Dong S, Hwang H. Diffusion scrubber-based field measurements of atmospheric formaldehyde and hydrogen peroxide. *Aerosol Science and Technology*. 1990;12(1):98-104.
 19. Lawson DR. The southern California air quality study. *Journal of the Air & Waste Management Association*. 1990;40(2):156-65.
 20. Sakugawa H, Kaplan IR. Observation of the diurnal variation of gaseous H_2O_2 in Los Angeles air using a cryogenic collection method. *Aerosol science and technology*. 1990;12(1):77-85.
 21. Seinfeld JH, Pandis SN. *Atmospheric chemistry and physics – from air pollution to climate change* (2nd ed.). John Wiley & Sons, Inc., Hoboken. 2006;674.
 22. Albinet A, Minero C, Vione D. Photochemical generation of reactive species upon irradiation of rainwater: Negligible photoactivity of dissolved organic matter. *Science of the total environment*. 2010;408(16):3367-73.
 23. Sakugawa H, Kaplan IR. H_2O_2 and O_3 in the atmosphere of Los Angeles and its vicinity: factors controlling their formation and their role as oxidants of SO_2 . *Journal of Geophysical Research: Atmospheres*. 1989;94(D10):12957-73.
 24. Mostofa KM, Sakugawa H. Spatial and temporal variations and factors controlling the concentrations of hydrogen peroxide and organic peroxides in rivers. *Environmental Chemistry*. 2009;6(6):524-34.
 25. Sakugawa H, Yamashita T, Kwai H, Masuda N, Hashimoto N, Makino S, Nakatani N, Takeda K. Measurements, and production and decomposition mechanisms of hydroperoxides in air, rain, dew, river and drinking waters, Hiroshima prefecture, Japan. *Chikyukagaku (Geochemistry)*. 2006;40:47-63.
 26. Yamada E, Tomozawa K, Nakanishi Y, Fuse Y. Behavior of hydrogen peroxide in the atmosphere and rainwater in Kyoto, and its effect on the oxidation of SO_2 in rainwater. *Bulletin of the Chemical Society of Japan*. 2002;75(6):1385-91.
 27. Willey JD, Kieber RJ, Lancaster RD. Coastal rainwater hydrogen peroxide: Concentration and deposition. *Journal of atmospheric chemistry*. 1996;25(2):149-65.
 28. Morris JJ, Johnson ZI, Szul MJ, Keller M, Zinser ER. Dependence of the cyanobacterium *Prochlorococcus* on hydrogen peroxide scavenging microbes for growth at the ocean's surface. *PloS one*. 2011;6(2):e16805.
 29. Lesser MP. Oxidative stress in marine environments: biochemistry and physiological ecology. *Annu. Rev. Physiol.* 2006;68:253-78.
 30. Tahara K. Study on the monitoring and source of pesticides in river water. M.Sc. Thesis, Hiroshima University (in Japanese). 2005;81.
 31. Mostofa KMG, Honda Y, and Sakugawa H. Dynamics and optical nature of fluorescent dissolved organic matter in river waters in Hiroshima Prefecture, Japan. *Geochemical Journal*. 2005;39:257–271.

How to cite this article:

Anifowose AJ., Olabode OA., Adedotun IS., Sakugawa H. Hydrogen peroxide measurements: its wet deposition in Higashi-Hiroshima city, concentration in Kurose River and role towards hydroxyl radical formation. *Research Journal of Health Sciences*, 2021, 9(4):

Table 1. The temperature, conductivity and pH in the rainwater and Kurose River in Higashi-Hiroshima city, 2013

Month (2013)	Rain water			Kurose River		
	Temperature (°C)	Conductivity ($\mu\text{S cm}^{-1}$)	pH	Temperature (°C)	Conductivity ($\mu\text{S cm}^{-1}$)	pH
2/Jan	6.7	9.57	5.40	12.6	225	6.89
18/Feb	3.5	20.9	5.40	13.9	147	7.49
13/Mar	12	27.8	4.50	18.7	214	7.61
24/Apr	12	11.5	4.67	18.4	229	8.09
19/May	16.5	7.69	6.40	24.2	328	7.08
26/June	20.5	5.36	6.30	21.4	111	6.95
July	na	na	na	28.8	251	6.28
24/Aug	24.5	4.25	6.36	28.6	351	6.19
Sep	na	na	na	20.7	225	7.15
23/Oct	17.4	3.05	6.32	18.6	131	7.40
25/Nov	10.5	6.48	5.92	9.7	215	7.65
26/Dec	5.5	42.5	5.71	8.7	218	7.38

na = not available due to unavailability of samples. River data for each month = average of six (6) stations.

Table 2. Concentrations of major anions and dissolved organic carbon (DOC) in the rainwater and Kurose River in Higashi-Hiroshima, 2013

Month	Rain water: anions (μM)					Kurose River: anions (μM)				
	NO ₂ ?	NO ₃ ?	SO ₄ ²⁻	Cl?	DOC	NO ₂ ?	NO ₃ ?	SO ₄ ²⁻	Cl?	DOC
Jan	0.40	10.0	13.8	9.0	61	6.71	96.5	523	703	161
Feb	0.38	14.5	18.4	7.3	47	3.27	56.3	227	362	150
Mar	0.08	17.6	45.7	31	157	7.97	83.6	482	699	186
April	0.30	10.6	12.3	9.0	46	6.98	67.1	502	591	216
May	0.21	9.50	7.40	17	109	15.2	87.3	737	1005	284
June	0.30	6.40	4.30	8.2	52	1.54	37.9	126	188	274
July	na	na	na	na	na	13.4	67.3	683	781	243
Aug	0.10	0.81	0.77	2.3	161	13.5	85.9	798	1062	312
Sept	na	na	na	na	na	11.6	70.6	402	685	181
Oct	0.12	3.90	2.11	1.8	46	2.58	41.8	180	264	156
Nov	0.23	5.23	8.17	6.1	37	5.16	67.0	372	611	162
Dec	1.36	35	69	40	89	6.09	69.2	369	619	143

na = not available due to unavailability of samples.

River data for each month = average of six (6) stations.

The DOC unit (μM) = $\mu\text{mol C L}^{-1}$

Table 3. Concentrations of major cations in the rainwater and Kurose River in Higashi-Hiroshima city, 2013

Month	Rain water: cations (μM)					Kurose River: cations (μM)				
	Na ⁺	K ⁺	Ca ²⁺	Mg ²⁺	NH ₄ ⁺	Na ⁺	K ⁺	Ca ²⁺	Mg ²⁺	NH ₄ ⁺
Jan	10.4	1.03	3	bd	32.1	1248	87	468	71	368
Feb	7.00	1.03	2.75	bd	37.1	1274	104	297	44	227
Mar	28.7	2.82	6	2.5	123	1056	75	263	49	201
April	4.80	0.77	bd	5	19.3	998	76	411	47	190
May	6.50	0.77	bd	bd	36.4	1397	118	654	76	191
June	12.9	0.54	4.6	0.4	16.4	396	46	257	45	66
July	Na	na	na	na	na	1217	100	591	66	161
Aug	3.12	0.25	0.56	bd	2.9	1522	107	99	63	186
Sept	Na	na	na	na	na	942	75	423	36	125
Oct	2.51	0.37	bd	bd	8.6	485	51	270	35	92
Nov	7.14	0.29	0.8	bd	17.9	895	73	423	49	186
Dec	116	3.08	94.5	2.5	12.1	913	71	401	48	220

na = not available due to unavailability of samples. bd = below detection.

River data for each month = average of six (6) stations.

Table 4. Hydroxyl radical ($\cdot\text{OH}$) measurements in the rainwater and Kurose River in Higashi-Hiroshima city, 2013

Month	Rain water				Kurose River			
	R _{OH} (10^{-11}M/s)	$\cdot\text{OH}_{\text{SRC}}$ (10^5 s^{-1})	[$\cdot\text{OH}$] _{SS} (10^{-16} M)	lifetime (μs)	R _{OH} (10^{-10} M/s)	$\cdot\text{OH}_{\text{SRC}}$ (10^5 s^{-1})	[$\cdot\text{OH}$] _{SS} (10^{-16} M)	lifetime (μs)
Jan	3.2	2.0	1.6	5.1	2.3	3.1	7.6	4.4
Feb	4.6	2.2	2.1	4.5	1.1	3.2	4.2	3.7
Mar	10	4.4	2.4	2.3	2.6	3.4	7.3	3.8
April	6.5	3.8	1.7	2.6	2.4	5.6	18	6.0
May	12	3.2	3.7	3.1	5.1	5.3	16	3.4
June	7.8	2.6	3.1	3.9	0.7	2.5	5.9	6.6
July	na	na	na	na	4.0	4.4	28	4.9
Aug	1.7	9.6	0.2	1.0	3.2	9.0	9.5	3.6
Sept	na	na	na	na	4.0	4.3	9.6	2.3
Oct	9.4	4.2	2.3	2.4	0.9	3.4	9.0	8.7
Nov	3.8	8.5	0.4	1.2	1.6	3.1	12	7.8
Dec	23.6	1.0	23	9.8	2.0	4.2	5.8	2.8

R_{OH} = $\cdot\text{OH}$ photoformation rate; $\cdot\text{OH}_{\text{SRC}}$ = $\cdot\text{OH}$ scavenging rate constant;

[$\cdot\text{OH}$]_{SS} = $\cdot\text{OH}$ steady-state concentration. na = not available due to lack of samples in those months.

River data for each month = average of six (6) stations

Table 5. Estimated contributions by H₂O₂ and other sources towards [•]OH photoformation rate (R_{OH}) measured in the rainwater and Kurose River in Higashi-Hiroshima city, 2013

Month	Rain: contribution (%)				River: contribution (%)			
	H ₂ O ₂	NO ₂ ?	NO ₃ ?	unknown	H ₂ O ₂	NO ₂ ?	NO ₃ ?	unknown
Jan	5.9	29	5.0	60	0.1	68	6.8	26
Feb	0.2	19	5.0	76	0.3	68	8.1	24
Mar	37	2	2.7	59	0.1	70	5.1	25
April	44	11	2.6	43	0.3	67	4.5	28
May	48	4	1.3	46	0.2	69	2.8	28
June	22	9	1.3	68	0.7	49	8.4	42
July	na	na	na	Na	0.4	78	2.7	19
Aug	32	14	0.8	53	0.1	80	3.5	17
Sept	na	na	na	Na	0.1	67	2.8	30
Oct	27	3	0.7	70	0.5	69	7.8	23
Nov	2.8	14	2.2	81	0.2	73	6.6	20
Dec	0.4	13	2.4	84	0.1	71	5.6	24

na = not available due to lack of samples in those months.

River data for each month = average of six (6) stations.

Rate constants for [•]OH formation from the H₂O₂, NO₂– and NO₃– photolysis in aqueous solution under sunlight ($J_{OH1H2O2}$, J_{OH1NO2} , J_{OH1NO3}), were 4.02×10^{-6} , 2.30×10^{-5} and $1.60 \times 10^{-6} \text{ s}^{-1}$, respectively (Takeda et al., 2004).

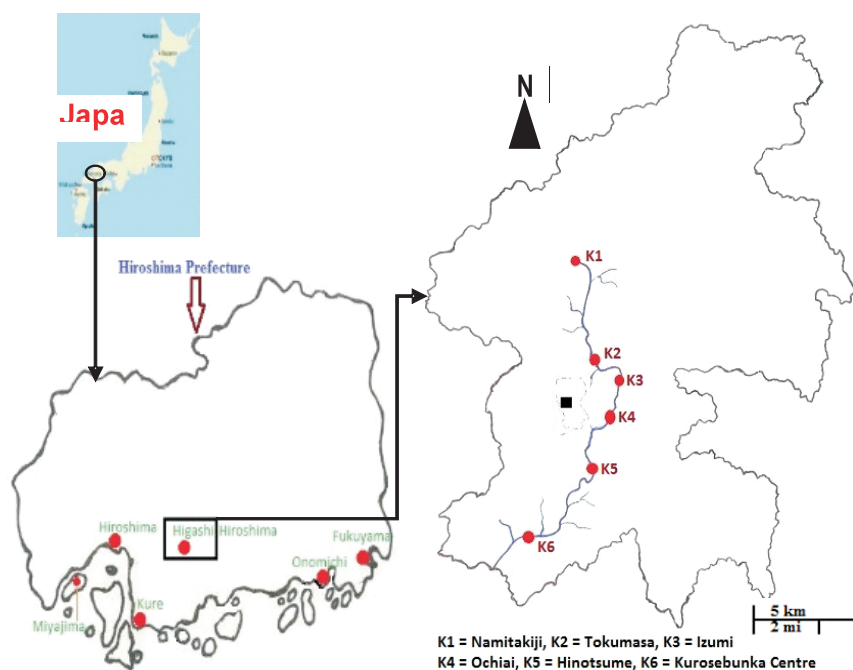


Figure 1. Map showing sampling locations of the rainwater (the black square) and in the Kurose River (K1–K6) in Higashi-Hiroshima city, Japan. The inscribed dotted line around the black square indicates the map of Hiroshima University

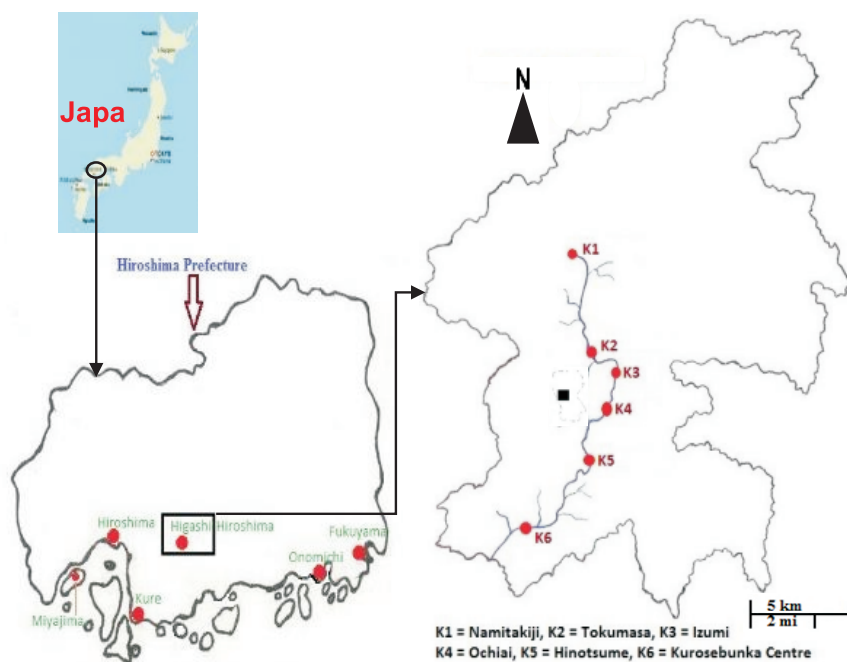


Figure 1. Map showing sampling locations of the rainwater (the black square) and in the Kurose River (K1–K6) in Higashi-Hiroshima city, Japan. The inscribed dotted line around the black square indicates the map of Hiroshima University

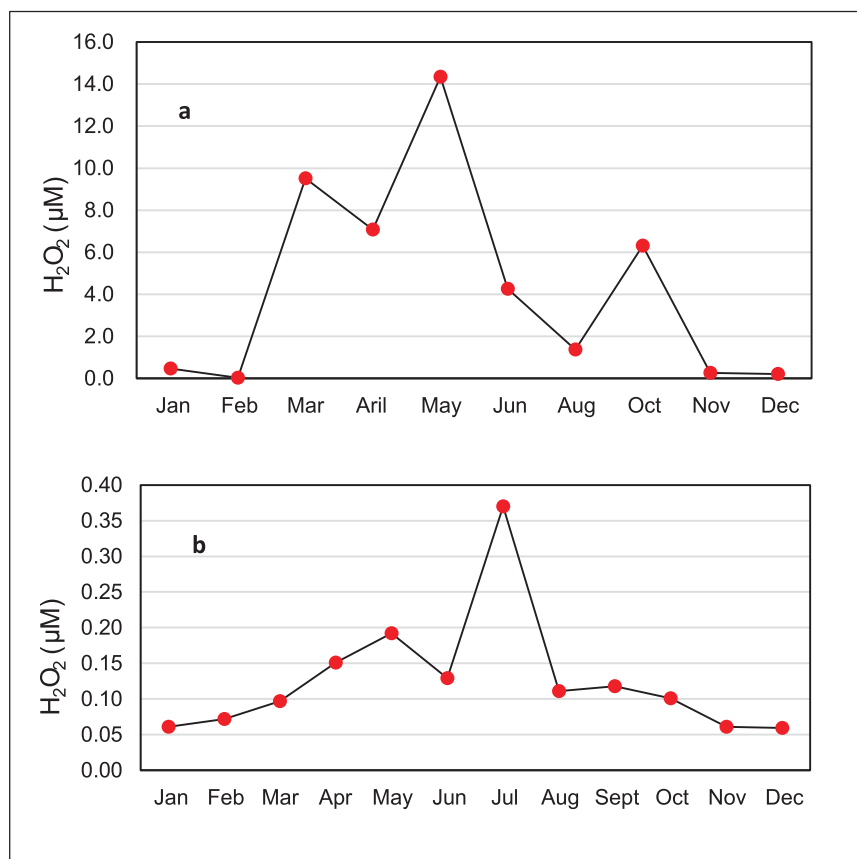


Figure 2. Monthly concentration of H₂O₂ in the rainwater (a) and Kurose River (b) in Higashi-Hiroshima city, 2013

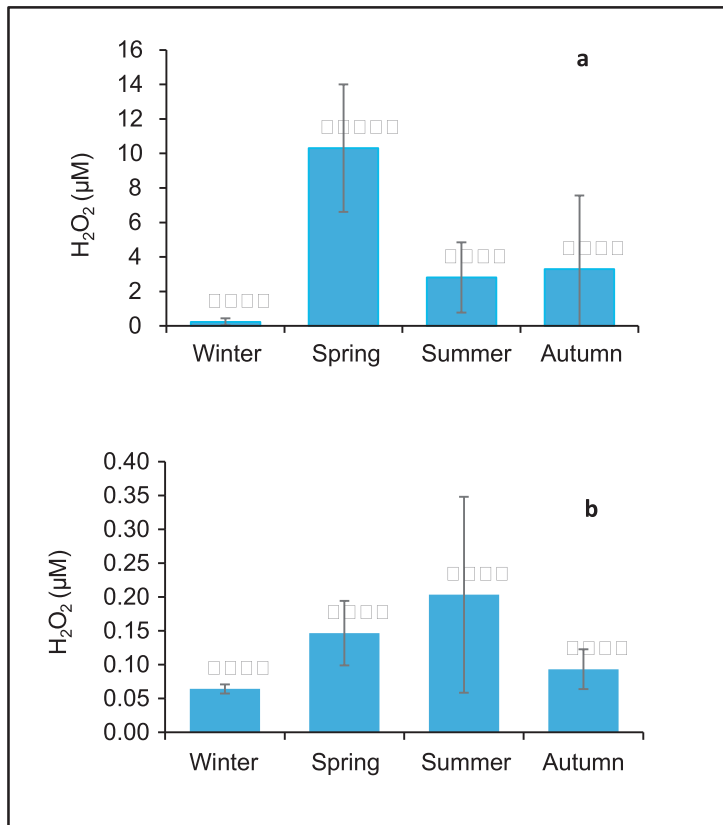


Figure 3. Seasonal variations of H₂O₂ in the rainwater (a) and Kurose River (b) in Higashi-Hiroshima, 2013 (winter: December–February; spring: March–May; summer: June–August; autumn: September–November)

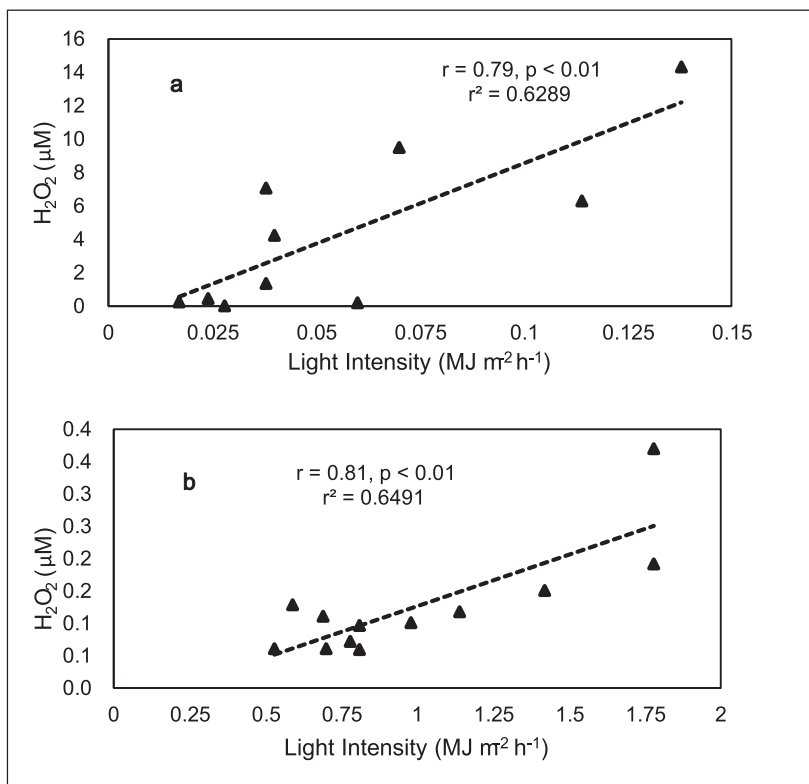


Figure 4. Monthly concentrations of H₂O₂ in rainwater (a) and Kurose River (b) as a function of the solar intensity in Higashi-Hiroshima city

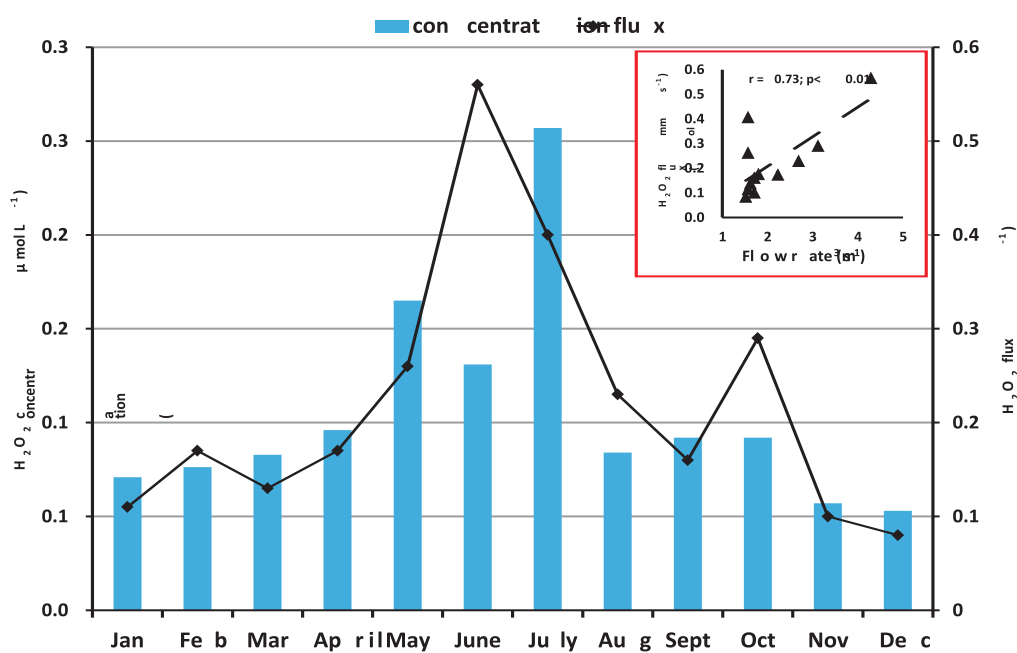


Figure 5. Concentration and flux of H₂O₂ at Hinotsume location, Kurose River, in 2013. Inset is the flux of H₂O₂ as a function of the river flow rate